Biochimica et Biophysica Acta 1862 (2016) 1650–1662

Contents lists available at ScienceDirect

Biochimica et Biophysica Acta

journal homepage: www.elsevier.com/locate/bbadis

Metabolite mapping reveals severe widespread perturbation of multiple metabolic processes in Huntington's disease human brain

Stefano Patassini [a,b,c,d,*], Paul Begley [c,d], Jingshu Xu [a,b,c,d,e], Stephanie J. Church [c,d], Suzanne J. Reid [a], Eric H. Kim [b,f], Maurice A. Curtis [b], Mike Dragunow [b], Henry J. Waldvogel [b], Russell G. Snell [a,b], Richard D. Unwin [c,d], Richard L.M. Faull [b,1], Garth J.S. Cooper [a,b,c,d,e,*,1]

[a] School of Biological Sciences, Faculty of Science, University of Auckland, Auckland, New Zealand
[b] Centre for Brain Research and Department of Anatomy with Radiology, Faculty of Medical and Health Sciences, University of Auckland, Auckland, New Zealand
[c] Centre for Advanced Discovery and Experimental Therapeutics (CADET), Central Manchester University Hospitals NHS Foundation Trust, Manchester Academic Health Sciences Centre, Manchester, UK
[d] Institute of Human Development, Faculty of Medical and Human Sciences, The University of Manchester, Manchester, UK
[e] Maurice Wilkins Centre for Molecular Biodiscovery, University of Auckland, Auckland, New Zealand
[f] Department of Pharmaceutical Sciences, Northeastern University, Boston, MA 02115, United States

ARTICLE INFO

Article history:
Received 7 April 2016
Received in revised form 31 May 2016
Accepted 1 June 2016
Available online 04 June 2016

Keywords:
Neurodegenerative disease
Huntington's disease
Polyol pathway
Brain urea metabolism
Metabolic brain disease
Inositol pathway

ABSTRACT

Huntington's disease (HD) is a genetically-mediated neurodegenerative disorder wherein the aetiological defect is a mutation in the Huntington's gene (HTT), which alters the structure of the huntingtin protein (Htt) through lengthening of its polyglutamine tract, thus initiating a cascade that ultimately leads to premature death. However, neurodegeneration typically manifests in HD only in middle age, and mechanisms linking the causative mutation to brain disease are poorly understood. Brain metabolism is severely perturbed in HD, and some studies have indicated a potential role for mutant Htt as a driver of these metabolic aberrations. Here, our objective was to determine the effects of HD on brain metabolism by measuring levels of polar metabolites in regions known to undergo varying degrees of damage. We performed gas-chromatography/mass spectrometry-based metabolomic analyses in a case-control study of eleven brain regions in short *post-mortem*-delay human tissue from nine well-characterized HD patients and nine matched controls. In each patient, we measured metabolite content in representative tissue-samples from eleven brain regions that display varying degrees of damage in HD, thus identifying the presence and abundance of 63 different metabolites from several molecular classes, including carbohydrates, amino acids, nucleosides, and neurotransmitters. Robust alterations in regional brain-metabolite abundances were observed in HD patients: these included changes in levels of small molecules that play important roles as intermediates in the tricarboxylic-acid and urea cycles, and amino-acid metabolism. Our findings point to widespread disruption of brain metabolism and indicate a complex phenotype beyond the gradient of neuropathologic damage observed in HD brain.

1. Introduction

Huntington's disease is an autosomal-dominant genetic disorder caused by an expanded CAG repeat in exon 1 of the HTT gene, which is located on chromosome 4 and encodes the huntingtin protein [1]. Clinically, HD manifests with a triad of symptoms, including progressive motor dysfunction, cognitive decline, and psychiatric disturbance with the age of onset inversely related to the repeat length [2,3]. The pathogenic mechanism causes marked degeneration of the caudate/putamen region and eventually more widespread loss of cortical, prefrontal, temporal, thalamic, cerebellar and hippocampal neurons with diffuse shrinkage of brain tissue [4].

Biochemical pathways in which alterations have been linked to expression of the mutant huntingtin protein (mHtt) are numerous, and include impaired maintenance of energy metabolism [5]. Indeed, HD-gene carriers can undergo marked weight loss despite sustained caloric intake, consistent with alterations in energy metabolism that contribute to the pathological process [6]. Interestingly, the mechanisms responsible for some of the metabolic abnormalities observed in HD have been considered as potential targets for developing biomarkers

* Corresponding authors at: Centre for Advanced Development and Experimental Therapeutics, Central Manchester University Hospitals NHS Foundation Trust, Manchester Academic Health Sciences Centre, Manchester, UK, M13 9WL.
E-mail addresses: stefano.patassini-2@manchester.ac.uk (S. Patassini), garth.cooper@manchester.ac.uk (G.J.S. Cooper).
[1] Equal contributions.

http://dx.doi.org/10.1016/j.bbadis.2016.06.002

for disease monitoring as well as potential therapeutic targets [7–9]. Although some studies have suggested beneficial potential of such drugs in improving aspects of the metabolic disturbances in HD, clinical trials have shown conflicting results [10,11]. The development of therapies aimed at improving the energy deficits in HD is challenging, since the heterogeneous distribution of metabolic defects in HD implies a complex interaction involving both CNS and extra-cerebral organ systems [12]. This complexity is exacerbated by the potential variation in metabolic perturbations between different brain regions in HD-gene carriers [13]. Although it is still uncertain exactly how CNS metabolism is influenced by the ubiquitously-expressed mHtt protein, it seems likely that different brain regions have a heterogeneous response to the consequent metabolic disturbance.

It is necessary to understand the metabolic pathways altered in HD in order to better understand the link between metabolic abnormalities and pathogenesis. To date, however, detailed knowledge of the metabolites contributing to these traits has been somewhat sparse. Nor is it known how these metabolic alterations contribute to pathology in distinct brain regions. Since few investigations into these aspects of HD pathogenesis have been reported to date, it is therefore valuable to address the following key questions: 1) to clarify whether metabolic perturbations are present in a substantial number of different brain regions in HD; 2) to determine whether putative defects represent common or unique metabolic signatures among the different regions of affected HD brain; and 3) to correlate those metabolite changes with the degree of regional tissue damage known to occur in HD brain.

In order to study the metabolic effects occurring in HD across different regions of affected brain, we chose to apply gas chromatography/mass spectrometry (GC–MS) to detect and characterise putative alterations in polar metabolite levels in a case-control approach in short *post-mortem*-delay brain tissue of patients and matched controls. To our knowledge, this is the first time that an untargeted GC–MS-based global metabolomic approach has been used to profile polar metabolite alterations in a large number of HD human brain regions. While metabolite analysis has been used to profile biofluids from individuals affected with HD (sometimes with conflicting results [14,15]), available human brain *post-mortem* studies are relatively few, because high-quality tissue is difficult to procure.

For this study, human-brain tissue was obtained from the Neurological Foundation of New Zealand Human Brain Bank, which has extensive experience in the characterization and storage of high quality brain samples [16,17]. Here, eleven regions of the human brain underwent metabolomic analyses in a case-control study. To accurately describe the metabolic impact of HD pathology, the regions selected were chosen to provide a comprehensive representation of the heterogeneous range of degeneration that occurs in HD brain. The putamen and motor cortex were included, as they are severely affected during the disease progression; sensory cortex, globus pallidus, cingulate gyrus, and substantia nigra were also included, since they are known to be moderately affected; lastly, hippocampus, entorhinal cortex, cerebellum, middle frontal gyrus, and middle temporal gyrus were also studied, as they have not been commonly linked to major neurodegeneration in this context [18,19].

2. Materials and methods

2.1. Acquisition of human brains

Whole brains from nine HD patients and nine matched controls were obtained from the Neurological Foundation of New Zealand Human Brain Bank at the University of Auckland. All procedures employed in this study were approved by the University of Auckland Human Participants Ethics Committee with informed consent from all families.

2.2. Human brain tissue

Each brain was dissected under the supervision of expert neuroanatomists who accurately identified and pre-dissected each of the brain regions studied (Suppl. Fig. 1). We obtained tissue from eleven identified regions: putamen, PUT; motor cortex, MCTX; sensory cortex, SCTX; globus pallidus, GP; cingulate gyrus, CG; substantia nigra, SN; middle frontal gyrus, MFG; middle temporal gyrus, MTG; cerebellum, CB; hippocampus, HP; and entorhinal cortex, ENT. Tissue samples of 50 ± 5 mg, were dissected from each region from each patient, and stored at −80 °C until analysis.

2.3. Tissue extraction

Aliquots of 50 ± 5 mg brain tissue underwent a Folch-style extraction using a TissueLyser bead homogeniser (Qiagen; UK). Each sample was extracted in 0.8 ml 50:50 (*v*/v) methanol:chloroform, to which a solution of the labelled internal standards (Citric acid-d_4, $^{13}C_6$-D-fructose, L-tryptophan-d_5, L-alanine-d_7, stearic acid-d_{35}, benzoic acid-d_5, and leucine-d_{10}) in methanol had been added to achieve a final concentration of 0.016 mg/ml of each internal standard in the extraction solvent, for 10 min at 25 Hz with a single 3-mm tungsten carbide bead. Samples corresponding to each brain region were handled as single separate batches for this and all subsequent procedures. Phase separation was achieved by addition of 0.4 ml water followed by vortex-mixing (10–15 s) and centrifugation (2400 g, 5 min), and subsequent removal of the chloroform layer. Extraction blanks were prepared by including tubes without tissue samples in each batch.

2.4. Sample preparation

From the methanol:water supernatant, 200-μl aliquots were transferred to pre-labelled tubes. For each brain region, quality control replicates (QC) were prepared pooling equal amounts of extract (200 μl) from each sample. After brief mixing, 200-μl aliquots of each sample were dried (30 °C, 16–18 h) in a Speedvac centrifugal concentrator (Thermo Scientific). Dried residues were then held in sealed tubes at 4 °C until derivatization for GC–MS analysis.

2.5. GC–MS analysis

The method used was based upon one that we previously described [20,21]. Briefly, this method uses methoximation and trimethylsilylation to generate a profile of polar small-molecule metabolites such as those corresponding to amino acids, simple organic acids and monosaccharides, and is typically applied to provide comparative data in a case-control experimental design [22].

Dried residues were reconstituted in 60-μl methoxylamine hydrochloride solution (20 mg/ml in dry pyridine) and heated at 80 °C for 20 min in sealed tubes. 60 μl of *N*-methyl-*N*-(trimethylsilyl) trifluoroacetamide (MSTFA) was then added and heating continued at 80 °C for a further 20 min. Finally, 10 μl of a retention-time marker solution (nine n-alkanes covering the range C12-C32 dissolved at 10 mg/ml in 1:1 hexane:pyridine) was added and the solutions transferred to autosampler vials for GC–MS analysis.

Chromatography was carried out using an Agilent/J&W DB17-MS column (30 m × 0.25 mm × 0.25 μm) with a 3 m × 0.25 mm retention gap, and helium carrier at a constant flow of 1.4 ml/min. Oven temperature was progressively increased from 50 °C to 300 °C at 10 °C /min. 1 μl injections were performed in Pulsed-Splitless mode using an MPS2 autosampler (Gerstel; Germany), and a 7890A Gas Chromatograph with Split/Splitless inlet (Agilent; USA). Column effluent was analysed using a Pegasus HT time-of-flight mass spectrometer (LECO; UK), acquiring 10 spectra/s over the mass range of 45–800 Da.

This study was performed in a series of single-batch experiments, wherein each specific brain region constituted a batch. Within each

batch, individual HD cases and controls were randomised, and run in a sequence interleaved with injections of the pooled QC samples and extraction blanks. Extraction blanks were inspected visually to confirm absence of carryover.

2.6. Data analysis

Data were prepared using the 'Reference Compare' method within ChromaTOF 4.5 (LECO). Databases we employed were: the NIST Mass Spectral Reference Library (NIST08/2008; National Institute of Standards and Technology/Environmental Protection Agency/National Institutes of Health Spectral 262 Library; NIST, Gaithersburg, MD, USA); and the Golm Metabolome Database (Max Planck Institute of Molecular Plant Physiology, Potsdam-Golm, Germany). Chromatographic retention-time data were available from our library reference standards. Matching of both mass spectra/expected retention time and peak-shape integration was manually verified by two independent investigators to constitute a definitive molecular identification. Pooled QC samples were chosen as representative of the human brain to generate a final list of metabolites. For all the brain regions analysed here the same reference list was used. In total 142 metabolite features were originally selected from the GC–MS chromatogram. After removal of duplicates (e.g. two isomeric peaks for glucose) and unidentified IDs, the remaining 63 identified metabolites were analysed and reported in this study. A representative GC–MS chromatogram is shown in Suppl. Fig. 2.

2.7. Statistical methods

Data analysis was performed by transforming the GC–MS raw data in $\log_{10}$ space. For each brain region a multivariate principal-components analysis (PCA) was performed on the entire metabolite list to assess the quality of the dataset generated (SIMCA-P; UMetrics AB). Statistical significance was calculated using multiple 2-tailed *t*-tests and corrected for potential effects of multiple comparisons by applying a false-discovery rate (FDR) 10% correction [23]. Fold-changes in metabolite abundances were calculated as the ratio of the mean of each group, and have been presented as HD group/control group ratios.

For each brain region, the potential effect of the mutant allele HTT CAG repeat size on brain metabolites was also investigated by generating pair-wise correlations between the number of CAG triplets versus the relative abundance of each metabolite ($\log_{10}$-transformed) in controls and HD groups using the statistical discovery software JMP® (Version 12.0.0; SAS). Since the number of cases analysed in this study is relatively limited, a conservative analysis was used in order to generate credible results. First of all, the values for each metabolite-CAG couple were visually depicted in a scatterplot matrix. Then, the strength of each correlation was verified by applying a simple bootstrap analysis. If the correlation coefficient (r) generated was in the range of r values >0.6 (or <-0.6) after bootstrap analysis, the determined metabolite-CAG pair correlation was considered reliable. Finally, a correlation was considered significant only if both r values and P-values were at least >0.8 (or <-0.8) and <0.01, respectively. Similar criteria were used to investigate the influence of age and *post-mortem* delay (PMD) on metabolite abundances in human brain.

3. Results

Here we measured the relative abundance of 63 well-defined metabolites in *post-mortem* samples from 11 brain regions from 9 patients with HD and 9 matched controls. Cases and controls were matched for male:female ratio, age, and PMD (Table 1). As expected, brain-weights were significantly lighter in cases than in controls ($P = 0.01$), consistent with late-stage disease. Lastly, HD cases were all heterozygotes for HTT mutations, with expanded polyglutamine tract-lengths ranging between 40 and 47 (Suppl. Table 1).

Table 1
Study-group characteristics.

Variable	Control	HD
Number	**9**	**9**
Male:female ratio	**6:3**	**6:3**
Age (y; ±95% CI)	**67.4** (60.0–74.9)	**65.2** (57.3–73.2)
PMD (h; ±95% CI)	**10.6** (8.1–13.1)	**11.2** (9–13.4)
Brain-weight (g; ±95% CI)	**1322** (1249–1396)	**1104** (938–1270)*

Data are means (±95% CI). Abbreviation: PMD, *post-mortem* delay.
* $P = 0.01$

The reproducibility of our GC–MS analysis was verified by monitoring the metabolite measurements of sample replicates (N = 5–7). In each brain region, limited technical variability was observed, even for low abundance metabolites, supporting the quality of the dataset generated (Suppl. Table 2; Suppl. Fig. 3).

To investigate whether the overall metabolite profile was different between HD and control brain, multivariate PCA analysis was performed for each brain region. As shown in Fig. 1, PCA analysis demonstrated a good class separation between HD gene-carriers and controls and the clustering of QC replicates suggests that technical variability is satisfactory in each brain region. Interestingly, a single HD case did not cluster together with either controls or HD cases. As clinical records did not indicate any valid reason for exclusion, we considered this patient as representative of the natural variability occurring in the HD human condition and therefore, the case was included in our subsequent analyses.

Following the assessment of sample quality and GC–MS reproducibility, the alterations in metabolite levels were investigated in HD brain. In total, 63 metabolites were monitored and 48 of these were significantly altered in abundance in at least one brain region. Among the metabolites identified as differentially abundant are key components of relevant biological pathways such as sugar metabolism, brain energy transduction, urea cycle, and amino-acid and nucleoside metabolism (Table 2; Suppl. Tables 3, 4). While the putamen (the region most affected by HD) showed the highest number of metabolites significantly altered in disease, the number of changes observed in other regions indicates a lack of correlation with the severity of pathology in HD brain (Fig. 2). Notably, polyol-pathway intermediates and amino acids were among those metabolite groups particularly affected in HD brain. In fact, marked accumulation of glucose, sorbitol and fructose was present in HD-mutation carriers, especially in those regions affiliated with the basal-ganglia loop; moreover, with the exception of the aromatic amino acids (tryptophan, tyrosine, and phenylalanine) and the relatively-obscure pyroglutamic acid, most other amino acids detected by our methodology tended to uniformly decrease in all brain regions examined. Similarly, the neurotransmitters gamma-aminobutyric acid (GABA) and its closely related precursor, 4-hydroxybutyric acid (GHB), are largely decreased in HD brain. These findings taken together, point to the existence of marked alterations in metabolism of amino acids and neurotransmitters in HD brain which require closer inspection. Thus, as metabolite interactions represent important components of biological processes, the study of how metabolic pathways generate or utilise these metabolites may help to elucidate the underlying molecular mechanisms in metabolic networks that contribute to the pathogenesis of HD [24,25].

To further investigate these perturbations in our study, an exploratory pair-wise Pearson-correlation analysis was performed using all the well-identified metabolites, and the results of controls and HD cases

Fig. 1. Principal component analysis (PCA) of the eleven human brain regions examined by GC–MS. PCA plots showing class separation in 11 brain regions of controls (*blue diamond*) and HD cases (*red diamond*). The relatively dense clustering observed between the QC measurements (*black cross*) supports the low variability and the good reproducibility of the GC–MS method applied for metabolite profiling in this study. The dimensions used for principal component analysis were PC1 and PC2.

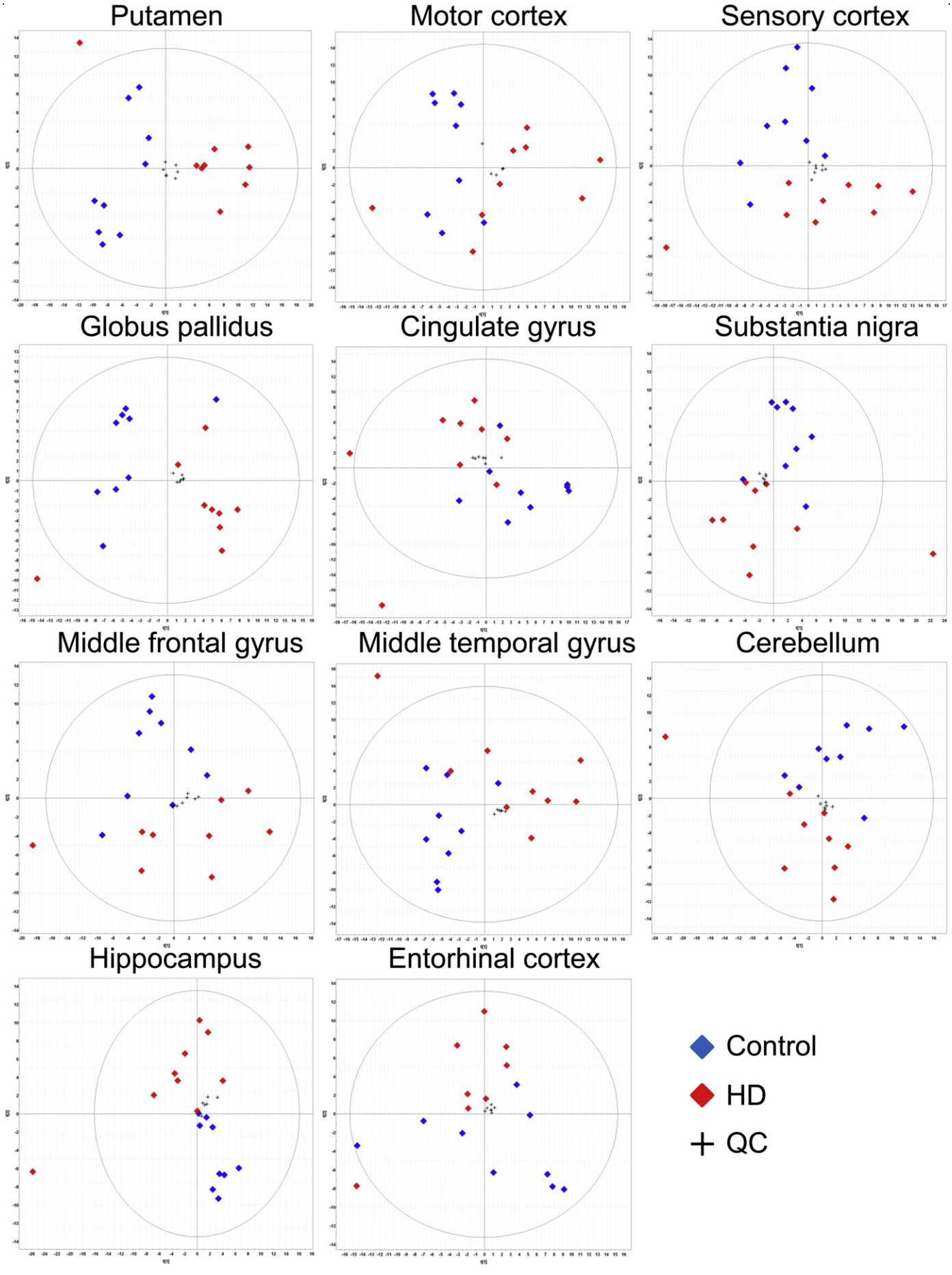
Putamen
Motor cortex
Sensory cortex
Globus pallidus
Cingulate gyrus
Substantia nigra
Middle frontal gyrus
Middle temporal gyrus
Cerebellum
Hippocampus
Entorhinal cortex
Control
HD
QC

Table 2
Group of metabolites altered in abundance across the eleven human brain regions in HD cases. The list of metabolites altered in abundance in the HD brain is showed here by separate classes. The values depicted in the table indicate the fold-change ratios of each metabolite in individual brain regions (HD group/control group). In bold are listed those metabolites statistically significant after being tested by multiple comparison analysis (FDR correction). Abbreviations: D, definitive (good mass spectral match and retention index confirmed by running authentic standard on our instrument under the same GC conditions as used for the study); C, confident (good mass spectral match to reference spectrum in NIST library for a compound with a "unique" mass spectrum); P, putative (good mass spectral match to NIST library for a compound with a "generic" mass spectrum).

Group of metabolites	PUT	MCTX	SCTX	GP	CG	SN	MFG	MTG	CB	HP	ENT
Glucose metabolites & pentoses											
Fructose (D)	**5.2**	2.4	2.8	2.4	2	1.9	2.2	2.6	**3.8**	2	2.6
Sorbitol (D)	**3.6**	2.9	**4.4**	3	1.9	2.8	**3.3**	2.6	2.8	1.7	2
Glucose (D)	**8.4**	2.3	**3.3**	**5.5**	1.9	**2.8**	2.3	1.6	2.2	1.7	1.8
Glucose-6-phosphate (D)	**13.1**	1.6	1.4	**6**	3.7	**5.1**	3	2.7	2.7	**3.4**	**7.7**
Alternative fuel source											
β-Hydroxybutyric acid (D)	**2.4**	1.9	3.1	1.8	2.1	**2.2**	2.3	2.6	1.9	**1.9**	2.1
Glycerol (D)	1	1	1	1.1	0.8	0.7	0.9	**0.7**	0.7	0.9	0.9
Threitol (D)	**1.7**	1.3	1.4	1.4	1.1	1.2	1.4	1.1	2.1	1.3	1.3
Glycerol-3-phosphate (D)	**2.3**	1.8	1.6	1.7	2.1	**2.6**	**3.1**	**3**	1.5	**2.2**	2.1
Glycerol-2-phosphate (P)	**1.7**	1.6	1.5	7	1.9	1.6	**2.2**	**1.9**	1.2	1.4	1.6
Scyllo-inositol (D)	1.2	0.8	**0.7**	1	0.8	0.8	0.9	**0.7**	**0.6**	**0.7**	0.6
Myo-inositol (D)	1.1	0.7	**0.8**	1.1	0.8	0.8	1	**0.7**	**0.8**	0.9	0.8
N-acetylglucosamine (C)	**2.1**	1.3	1.1	1.7	0.8	1.2	1.1	1	0.9	0.8	1.1
Ribitol (D)	**0.5**	0.6	**0.6**	0.7	0.6	**0.6**	0.8	0.7	0.6	**0.7**	0.7
TCA & Urea cycle and related											
Fumaric acid (C)	**2**	**2**	1.5	**1.5**	1.4	1.4	**1.8**	1.5	1.7	1.3	1.5
Citric acid (D)	1.1	1	1.2	1	1.2	**1.5**	1.3	1.2	1.2	1	0.9
Malic acid (C)	**2.1**	1.1	1.4	1.2	1	1.2	0.9	1.1	1.4	0.6	0.8
Urea (D)	**4.8**	**4.1**	**4.2**	**4.6**	**4.2**	**4.5**	**3.9**	**4.2**	**4.4**	**4.4**	**3.9**
Ornithine (D)	**0.5**	0.6	0.6	**0.6**	0.6	0.6	0.5	0.9	1	**0.4**	0.5
N-acetylglutamic acid (D)	1	0.8	**0.6**	1	0.7	0.8	0.8	0.9	0.8	0.7	0.8
Creatinine (D)	**0.8**	0.9	0.9	0.9	0.9	0.9	1	0.7	0.8	0.8	0.8
Amino acids											
Glycine (D)	**1.6**	0.9	0.7	0.6	1	1.1	0.8	0.6	**0.3**	0.6	0.8
Leucine (D)	0.8	0.8	0.9	0.8	0.8	0.7	0.7	0.9	**0.5**	**0.5**	0.7
Isoleucine (D)	0.8	0.8	0.7	0.7	0.7	0.7	0.6	0.6	**0.5**	**0.5**	0.7
Serine (D)	**0.6**	0.6	**0.6**	0.6	0.6	**0.5**	0.8	**0.5**	**0.4**	**0.5**	0.5
Threonine (D)	0.8	0.6	0.7	0.8	0.7	**0.6**	1	**0.6**	**0.6**	**0.5**	0.6
Aspartic acid (D)	**0.6**	1.3	0.9	0.7	0.7	0.7	0.9	0.9	0.8	0.8	0.8
Methionine (D)	1.2	1	0.9	1	0.9	0.9	0.9	0.9	0.6	**0.6**	0.7
Pyroglutamic acid (D)	**1.6**	1.1	1.1	1.4	1.1	1.4	1.3	1.3	1.1	1	1
Phenylalanine (D)	**1.6**	1.5	1.2	1.2	1	1.1	1.2	1.5	0.9	0.8	1.1
Proline (D)	**0.4**	0.5	**0.4**	0.5	0.4	0.6	0.4	0.5	**0.3**	**0.3**	0.4
N-acetylaspartic acid (D)	**0.7**	0.8	**0.8**	1	0.8	0.8	0.9	0.9	0.9	0.9	0.8
Lysine (D)	**0.6**	0.7	0.7	**0.6**	0.6	0.6	**0.5**	0.7	0.4	**0.4**	0.5
Tyrosine (D)	**1.8**	1.3	1.2	1.2	1.2	1.1	1	1.4	0.6	0.8	1.1
Tryptophan (D)	**1.7**	1.3	1.2	1.4	1.2	1.1	1.5	1.5	1.3	1	1.1
Glutamate (D)	1	1.1	1	**1.3**	0.9	0.9	1.1	0.9	1	1.1	0.8
Nucleosides											
Uracil (C)	**0.6**	0.8	0.8	0.7	0.8	0.8	0.8	0.7	0.6	**0.7**	0.8
Hypoxanthine (D)	**0.7**	0.7	**0.7**	0.8	0.7	**0.7**	0.6	**0.6**	**0.6**	**0.7**	0.8
Guanosine (D)	1.4	3.5	2.4	0.8	1.5	0.7	**4.5**	0.9	1	0.9	1.7
Xanthine (C)	**2.8**	**7.4**	2.6	1.5	1.8	1.3	1.8	1.1	1	1	1.7
Inosine (C)	**2.6**	1.6	1.2	1.8	1.1	0.9	1.5	0.8	1.2	1	1.2
Miscellaneous											
Ethanolamine (D)	**0.6**	0.8	0.8	0.7	**0.5**	**0.6**	0.6	**0.5**	**0.5**	**0.5**	0.6
Phosphoric acid (D)	**0.8**	**0.6**	**0.7**	1	**0.7**	**0.6**	0.8	**0.6**	**0.7**	0.8	0.7
GABA (D)	**0.5**	0.7	**0.7**	0.7	0.6	0.7	0.9	0.8	**0.7**	0.8	0.9
4-Hydroxybutyric acid (C)	**0.6**	0.7	0.5	**0.2**	0.3	0.4	0.7	0.5	**0.3**	0.6	0.6
Vitamin B5 (D)	**0.5**	0.6	0.5	**0.4**	0.5	**0.4**	0.6	0.6	0.6	**0.5**	0.6
Glutaric Acid (D)	2	0.6	0.8	**3**	0.8	0.9	0.8	0.8	0.9	0.8	0.8
Ethylene glycol (C)	0.6	0.7	1	0.6	0.3	0.6	**0.2**	0.7	0.5	0.6	0.5
Sugar phosphate (C)	**2.1**	1.4	1	1.6	1.1	1.2	2	1.1	0.9	1	1.1

compared for each brain region (Fig. 3). While some differences were present between the eleven brain-regions analysed for each group, a repeated pattern of correlated metabolites was noted in controls and HD cases, respectively. In controls, many of the metabolite-pairs found to be strongly correlated were participants or products of pathways related to amino-acid metabolism. These included leucine, isoleucine, serine, threonine, aspartic acid, methionine, phenylalanine, proline, lysine, tyrosine and tryptophan, as well as 4-hydroxybutyric acid. Notably, while most of the amino acids seem to be co-regulated in the control cases, a small group of amino acids, namely glutamine, alanine, beta-alanine, cysteine and valine, were found to be not correlated with any other amino acid in the same brain regions. New or additional strong correlations were observed between pairs of metabolites that participate in carbohydrate metabolism, amino-acid metabolism, and other processes linked to energy supply in the HD cases (Fig. 3).

To determine how mHtt polyglutamine tract-lengths might influence regional levels of brain metabolites, we investigated whether any correlation existed between the number of HTT CAG repeats and metabolite abundance in controls and HD cases. As the numbers in each group were relatively low, only those metabolites showing a

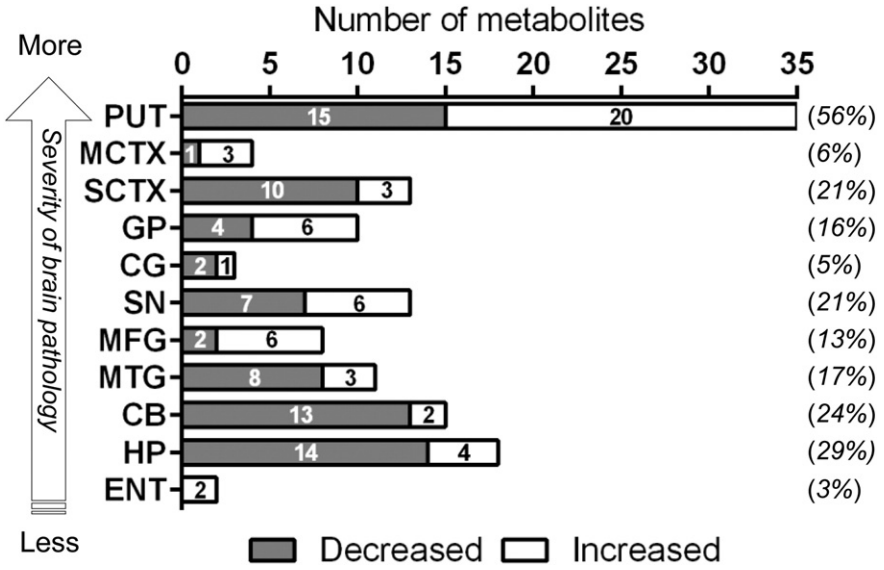

Fig. 2. Number of altered metabolites in HD brain in each brain region. Graph showing the number of metabolites decreased (*grey*) and increased (*white*) for each brain region. The areas analysed were ranked in the graph from the most to the least severely affected by degeneration in HD (i.e. from putamen to entorhinal cortex). The values showed on the right of the graph bars represent the number of altered metabolites in each brain region expressed as the percentage of the total 63 metabolites identified and quantified by GC–MS in this study.

robust correlation with HTT CAG size (r values >0.8 or <−0.8 with corresponding P-values of <0.01) were considered significant. Based on this criterion, 5 metabolites were pin-pointed whose concentrations strongly correlated with HTT CAG-repeat number: these were malic acid and *N*-acetylglutamic acid in the control group, and myo-inositol, glycine, and *N*-acetylaspartic acid in the HD group (Suppl. Table 5). Notably, these significant correlations were limited to those brain regions known to undergo severe degeneration in HD (Suppl. Table 5).

As striatal volume loss is known to correlate with HTT CAG-repeat number in both premanifest and manifest HD [26,27], the finding of myo-inositol ($r = 0.82$; $p = 0.007$) as the only metabolite strongly associated with the pathological HTT CAG length in putamen merits further investigation (Suppl. Fig. 4). A similar analysis was also performed to determine whether any significant correlation existed between the abundance of measured metabolites and the age/PMD of the cases studied. Taken together, our data indicate that neither age nor PMD influenced the metabolite abundances reported here (data not shown).

4. Discussion

Here we report our metabolomic analysis of human tissue from eleven different brain regions from HD cases and matched controls, to determine how metabolite levels might be differentially regulated in different regions of disease-affected brain. This is the first time, to our knowledge, that an untargeted GC–MS-based global profiling analysis of a large number of human-brain regions has been reported in HD. Furthermore, we have also undertaken detailed mapping of the metabolite alterations in specific brain regions in HD.

PCA analysis of the eleven brain regions showed minimal overlap between the control and HD cases, suggestive of a widespread, severe global effect of the HD mutation and/or downstream disease processes on brain metabolism. Moreover, several imaging studies have supported the view that there is a widespread effect on brain metabolism in HD mutation-carriers [28,29]. However, the greater metabolite group separation observed here in the putamen indicates that a more severe metabolic perturbation has taken place in this brain region in HD, consistent with the observed degree of pathological change.

Interestingly, the pattern of metabolite changes identified in this study does not correlate well with the gradient of degeneration commonly observed in *post-mortem* HD brains [30]. Surprisingly, whilst the putamen is pathologically the most affected area, the hippocampus and the cerebellum were among those regions wherein high numbers of metabolite alterations were observed. Volume loss is not commonly associated with the hippocampus and the cerebellum, however cerebellar and hippocampal pathology has been reported in both juvenile-onset and adult-onset HD [31–34]. Another unexpected result was the small number of changes in metabolite abundance in HD motor cortex.

Here we found several important processes to be altered in HD brains, including glucose and the polyol-pathway intermediates, sorbitol and fructose along with metabolites implicated in brain energetics, TCA cycle, urea cycle and amino acid metabolism. Brain energy supply is known to be dysfunctional in HD [35–38]. For example, PET studies indicate that glucose consumption is reduced in the basal ganglia of HD gene-carriers, even at the premanifest stage [39,40]. In our study, we observed a marked accumulation of glucose in the basal ganglia as well as those brain regions closely related to this circuit: these results indicate impaired glucose utilization in these regions in HD. Notably, of the eleven brain regions analysed here, putamen was the sole region where the concomitant upregulation of glucose, sorbitol and fructose was observed. To our knowledge, this is the first report showing increased levels in HD of all three sugars comprising the members of the polyol pathway. In the brain, sorbitol and fructose are commonly formed from glucose via the polyol pathway in astrocytes and neurons [41] and alterations of this pathway are generally associated with hyperglycaemia resulting from diabetic complications and have more recently also been demonstrated in the brain associated with Alzheimer's disease (AD) [42]. As over-activity in the polyol pathway may generate cell damage via osmotic stress or chemical toxicity of glucose and fructose, our results indicate that this mechanism may well act as a potential player in the profound neurodegeneration observed in the putamen in HD [43]. While it is unclear to date how mHtt might cause excessive activation of the polyol pathway in the HD putamen, it would be valuable to determine whether equivalent over-activation of the polyol pathway is also evident in the in vitro and in vivo animal models where a human HD mutation is expressed.

Further evidence of dysfunctional energy utilisation in the HD brain is also provided here by alterations in the levels of alternative fuel substrates such as threitol, glycerol, ribitol, glycerol-3-phosphate, glycerol-2-phosphate, and their derivates. These metabolites are commonly associated with essential metabolic pathways used as secondary energy sources in human tissues. Further indications are provided by the alterations observed in those metabolites known to participate in

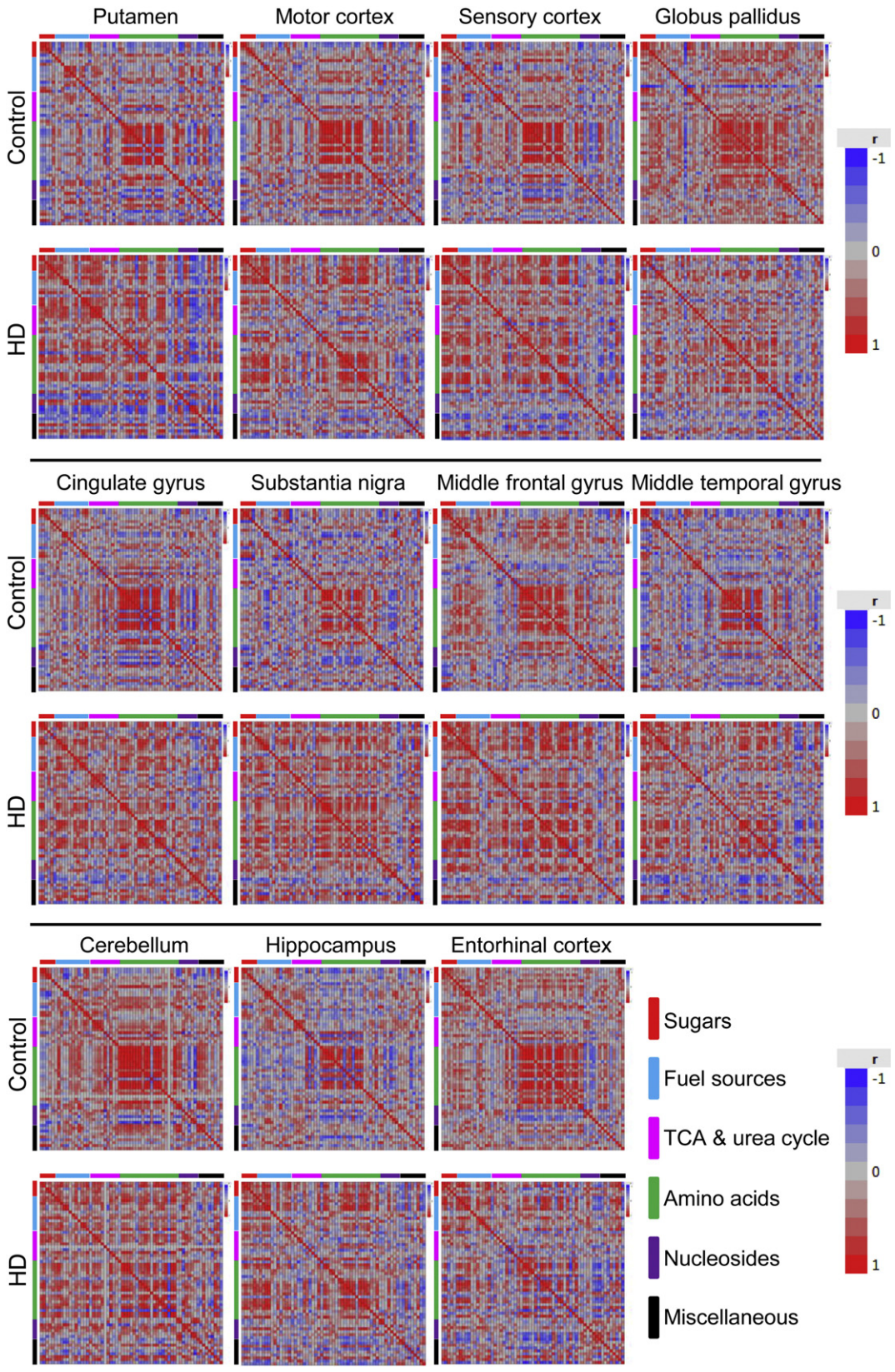

Fig. 3. Correlation heatmaps of metabolite co-regulation in control and HD cases in individual brain regions. Heatmaps illustrating the alteration in metabolite abundance co-regulations in controls (*top panel in each brain region*) and HD cases (*bottom panel in each brain region*). Differences between metabolite abundance co-regulations in controls and HD gene-carriers were investigated by pair-wise correlation analyses and reported in the above heatmaps as one of the colours of the Pearson correlation coefficient (r) gradient scale (*on the right*). As illustrated at the bottom of each heatmap in the panel, the metabolites considered for correlation analyses were separated by classes: sugars (*red*), fuels (*cyan*), TCA and urea cycle intermediates (*magenta*), amino acids (*green*), nucleosides (*purple*) and others (*black*).

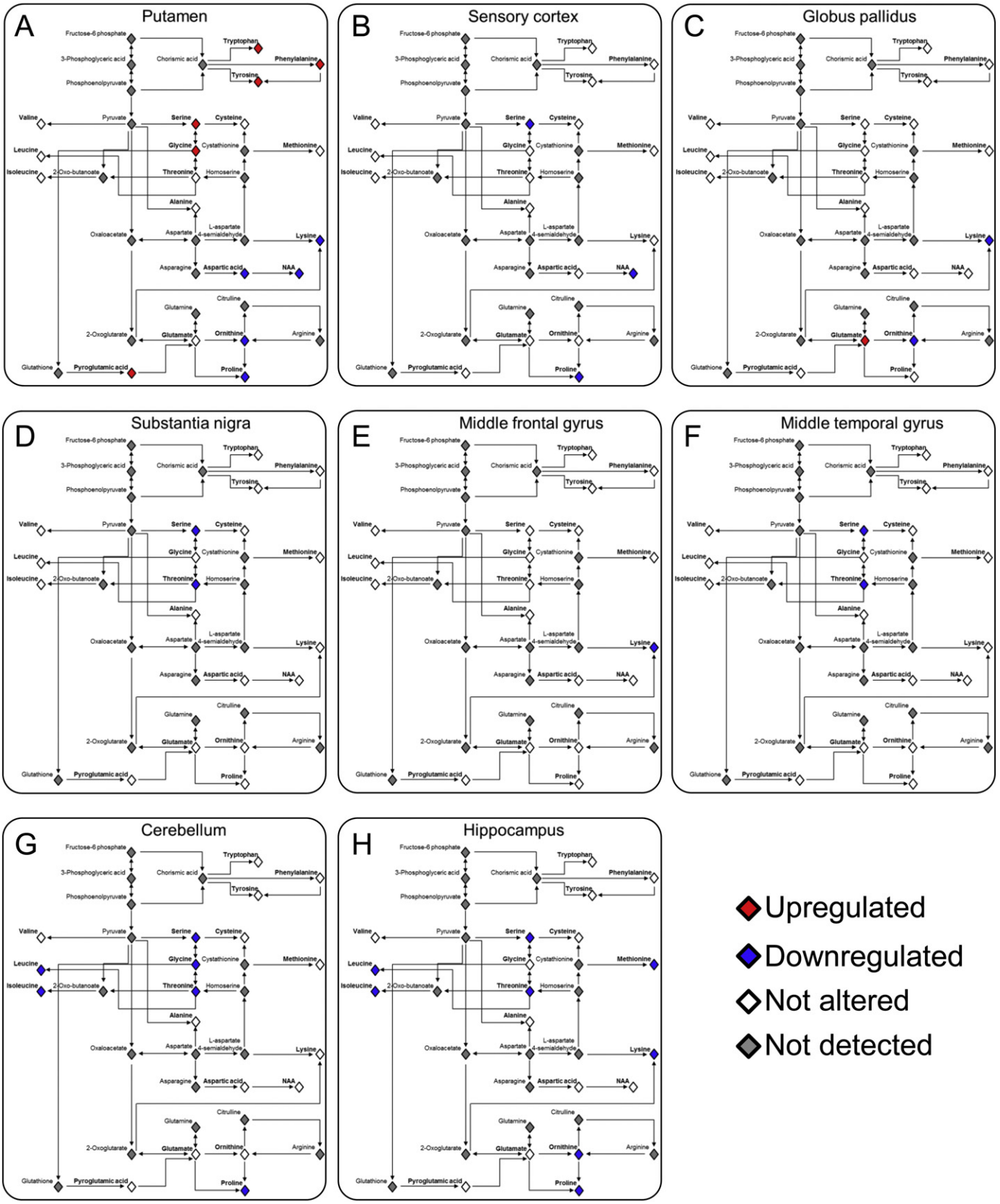

Fig. 4. Amino acid alterations in individual regions of the HD brain. A simplified diagram illustrating the relationships between amino acids detected in this study. (A–H). Each panel summarises the significant amino acid changes observed after correction for multiple comparisons in individual HD-brain regions as compared to controls. The abundance of tryptophan, phenylalanine and tyrosine is solely increased in putamen (A) and in none of the other brain regions examined by GC–MS (B–H). Legend: amino acids increased in abundance in HD (*red diamond*); amino acids decreased in abundance in HD (*blue diamond*); amino acids not altered in abundance in HD (*white diamond*); metabolites not detected by our GC–MS method (*grey diamond*). Abbreviations: NAA (*N*-acetylaspartic acid).

energy production. Here, most TCA-cycle intermediates detected by our GC–MS assay are increased in HD, particularly in the brain regions most severely affected in the disease. Taken together these observations point to a 'hypometabolic' state in the HD brain coupled to a reactive catabolic response. For instance, as a result of impaired glucose uptake in the brain, human organs can use alternative energy sources including ketone bodies, amino acids, or fatty acids in order to maintain nutrient flow into the TCA cycle. β-hydroxybutyric acid (βHB), a main ketone body, is generally produced in the liver during ketosis [44], and is utilised in the brain as an alternative fuel source for acetyl-CoA oxidation in the TCA cycle when glucose supply is deficient or perhaps metabolism is dysregulated as occurs in HD, AD and Parkinson's disease (PD) [39,42,45,46]. As βHB concentration is increased only in a limited number of the HD brain regions, our data indicates that this ketone may not be primarily used as a glucose-replacing substrate for energy production in the HD brain: these findings would also seem to exclude the possibility that the HD cases studied here were subjected to an overall ketotic state driven by putative alterations of the hepatic metabolism [47–49].

Amino-acid degradation is another biochemical mechanism that can provide substrates for the TCA cycle in order to sustain energy demands [50]. Here we found major decreases in several classes of amino acids in the brain of HD mutation-carriers. Among these were: the ketogenic amino acids lysine and leucine; the glucogenic amino acid methionine; and the ketogenic/glucogenic amino acids isoleucine and threonine. Notably, these amino acids can serve as primary fuel sources for mitochondrial oxidation via acetyl-CoA and succinyl-CoA, two of the key intermediates of the TCA cycle. While is not possible to establish the origin of these tissue metabolites in our study, we hypothesise that the decrease in amino acids observed here could reflect the need in HD brain for substrates to funnel into the TCA cycle: Similar mechanisms have been advanced to account for the diminished levels of branched-chain amino acids (BCAAs) found in plasma of HD gene-carriers [51].

Finally, the β-oxidation of fatty acids is also considered to provide an alternative source to glucose for energy production in the CNS via the TCA cycle. A number of reports indicate that a part of total energy requirement of the brain is usually fulfilled by oxidation of fatty acids [52–54]. As only the polar components of brain extracts were analysed for the current study, it is uncertain how fatty acids contained in our HD samples were affected. Nevertheless, the involvement of fatty-acid β-oxidation-related metabolites is believed to contribute to the HD-phenotype signature [14].

In light of these findings, we hypothesise that the accumulation of TCA cycle-intermediates observed here in some HD-brain regions may be indicative of increased oxidation of locally-generated or peripherally-derived fatty acids. Alternatively, the accumulation of TCA cycle- intermediates may result from an acquired impairment in the functionality of the enzymes that catalyse the component reactions that comprise the cycle, thus converting these metabolites into their final products and extracting chemical energy. Consistent with this observation, a number of studies have shown that several of the enzymes which participate in the chemical reactions of the TCA cycle are functionally impaired in HD [55].

The severe, global accumulation of urea in all brain regions of HD gene-carriers previously reported from this cohort have potential implications and the main outcomes are discussed elsewhere [56]. Nevertheless, further findings reported here shed light on the potential involvement of the urea cycle in HD pathogenesis. For instance, ornithine, a key intermediate of the urea cycle produced by cleavage of arginine by arginase to form urea, is predominantly decreased in the HD brains analysed here. Altogether, the decrease in ornithine levels is concomitant with the massive accumulation of urea in HD cases, pointing to a deficiency in the brain-urea clearance system rather than an impaired functionality of the urea cycle itself; this is consistent with observations reported by others [57]. On the other hand, this decrease in ornithine with accompanying urea accumulation could result from enhanced activity of two of the key enzymes of polyamine synthesis, namely arginase 1 (ARG1) and ornithine decarboxylase (ODC). Previous studies have shown that pathologically-elongated polyQ-proteins can boost the activity of ARG1 and ODC, leading to enhancement of polyamine production and ultimately to cell death [58]. This mechanism could be reflected at the functional level in our current data, with increased rates of conversion of arginine by ARG1 to ornithine and subsequently urea. An accumulation of ornithine is not observed here since our study provides a snapshot of metabolite concentration, not metabolic flux through a pathway, and ornithine can be rapidly converted by ODC to a primary substrate for polyamine synthesis. Further studies measuring the flux through this pathway in HD should be performed to test this hypothesis.

One of the most interesting findings reported here is the distinctive amino-acid signature observed in HD putamen. Indeed, this is the sole brain region where a group of amino acids sharing a common precursor were substantially increased in HD cases. The list of these includes the aromatic amino acids tryptophan, phenylalanine and tyrosine (Fig. 4; Suppl. Fig. 5).

Tryptophan is an essential amino acid that is closely linked to neuronal survival and immune- system regulation, among other processes [59,60]; furthermore, it serves as a key substrate for kynurenine-pathway metabolism [61], and its consumption is thought to be locally regulated in the brain, as most of the kynurenine-pathway intermediates do not readily cross the blood-brain barrier [62]. Therefore, we hypothesise that the conversion of tryptophan to kynurenine, mediated by the immune-inducible enzyme indoleamine 2,3-dioxygenase (IDO), might be dysfunctional in the HD putamen, resulting in tryptophan-accumulation in this region. While we cannot rule out tryptophan levels being reflective of a systemic imbalance in HD [63–65], in the present study, in contrast to others [66], our results are indicative of a brain region-specific accumulation of this metabolite in HD gene-carriers. Further studies will be necessary to clarify this apparent discrepancy.

The other two aromatic amino acids increased in the HD putamen, namely phenylalanine and tyrosine, represent the most important sources of catecholamines in the body and have been previously associated with peripheral pathogenesis in HD [49,67]. As phenylalanine is the main substrate for production of tyrosine via a non-reversible reaction catalysed by phenylalanine hydroxylase, the localised increase in tyrosine levels might be reflective of an elevated presence of phenylalanine in HD putamen. Phenylalanine is an essential amino acid assimilated by the body through diet and its excessive accumulation is causative of phenylketonuria (PKU), a genetic disease known to induce brain damage and mental illness in patients [68]. Notably, it has been suggested that PKU might recapitulate some aspects of amyloid disorders such as AD and PD [69]. Taken together, our data support a deeper investigation into the putative role of phenylalanine in HD pathogenesis, especially as phenylalanine intake can be easily controlled by diet [70].

It should be also noted that purine metabolism is significantly affected in HD cases in the current study. While hypoxanthine is decreased in most of the brain regions examined, guanosine, xanthine and inosine presented heterogeneity of distribution throughout the HD brain. These three purines are included in the short list of metabolites with higher %CV values upon analysis of replicate samples: as such their regulation in the HD brain should be interpreted with care. Nevertheless, the observation of altered purine metabolism in CNS could be related to the peripheral dysregulation of purine metabolites reported by others in HD [71].

Phosphatidylcholines (PCs) are the most abundant phospholipids in the CNS and play a primary role in the biosynthesis of new neuronal membranes and formation of synapses [72]. Ethanolamine serves as important substrate for the production of PCs via the Kennedy pathway [73] and is uniformly decreased in many of the HD-brain regions examined here, namely CG, SN, MTG, CB and HP where neuronal loss is not prominent. On the other hand, another study has shown that ethanolamine decrease is greater in more severely affected HD-brain regions [74]. Apart from the putamen, where similar findings were observed,

and the frontal cortex, where it is uncertain which portion of the large frontal lobe was used for analysis, these authors did not measure ethanolamine levels in the other brain regions reported here. Taken together, our results are consistent with synaptic/membrane dysfunction in HD [75–77] and suggest that these impairments might be not localized but widespread throughout the HD brain.

A number of studies have shown how neurotransmitter levels are commonly altered in neurodegenerative diseases [42,78,79]. To investigate this phenomenon, the levels of GABA, the primary inhibitory neurotransmitter in the CNS, were measured. As anticipated by other reports, GABA levels are generally decreased in HD cases when compared to controls [80] whereas the abundance of GHB was reportedly lower in HD cases in multiple brain regions, thus conflicting with previous studies [81]. The major difference in *post-mortem* delay between the cases used here (6.5–15 h) and in the other studies (22–72 h) might be in part responsible for the discrepancy observed.

Scyllo-inositol, an isomer of inositol, was reduced in most HD-brain regions examined here. These results are consistent with dysfunctional functionality in the inositol-phosphate pathway in HD brain. Notably, scyllo-inositol has been found to lower the accumulation of amyloid-β peptide in vivo [82] and α-synuclein and mHtt aggregates/mHtt protein in vitro [83,84]. In HD cells, the clearance mechanism is reportedly mediated by proteasomes and lysosomes, which promote mHtt aggregation and protein degradation [84]. Our results might therefore suggest that scyllo-inositol is involved, along with other factors, in the modulation of clearance-activation mechanisms in a compensatory response to mHtt aggregate-formation and polyQ-Htt accumulation in HD brain.

The presence of altered inositol phosphate metabolism in HD is also supported by changes in myo-inositol levels. In the CNS, myo-inositol represents 90% of total inositol and can be readily interconverted to scyllo-inositol [85]. This metabolite is often considered a marker of gliosis and is commonly monitored by magnetic resonance spectroscopy (MRS) [86,87]. However, the validity of myo-inositol as a gliosis-marker is yet to be proven [88] and there is still little agreement about how its levels are perturbed in HD [89,90]. In the present study, our results point to a broad decrease in myo-inositol in multiple brain regions in HD cases. The differences in sample size, brain region dissected, HD severity and the method applied might in part be responsible for the observed dissimilarities between our study and other reports [89,90]. Changes in myo-inositol levels are not solely associated with gliosis in the CNS, but may also be indicative of tissue-osmolality disequilibrium [91,92], as this metabolite acts as an organic osmolyte that participates in cell-volume regulation [93,94]. For instance in hepatic encephalopathy, brain myo-inositol depletion has been shown to counteract the astrocyte swelling caused by intracellular accumulation of glutamine in response to hyperammonaemia [95–99]. Notably, hyperammonaemia and other urea cycle-related defects have been associated with HD [100]. Taken together, the observed myo-inositol decrease could be indicative of a compensatory mechanism triggered by HD-damaged cells to counteract increased brain-ammonia levels. In light of this observation, it will be of interest to measure ammonia levels in suitably-prepared *post-mortem* HD brain. Finally, as the accumulation of myo-inositol seems to correlate with the degree of HTT CAG-repeat expansion in the putamen, we suggest that a direct link might exist between HTT mutation length, the inositol phosphate pathway, tissue osmolality and the severity of neurodegeneration in HD.

Since there are few comparable metabolite-profiling studies on human brains affected by neurodegenerative disorders available in the literature, our ability to discriminate between disease-specific HD phenotypes from those identified as a consequence of generalised neurodegeneration have been hampered to date. Furthermore, the capability of comparing across different metabolite studies is also complicated by a number of variables, such as mode of specimen collection and storage, sample preparation, the exact methodology used, and criteria applied for data analysis. To overcome some of these limitations, our group, in parallel with the present study, has also performed detailed metabolite profiling of *post-mortem* AD brains [42]. Since both studies shared the same source of samples (i.e. human brain bank, University of Auckland), similar classes of brain regions analysed, and the same GC–MS methodologies/data processing applied, we believe that the qualitative comparison of these valuable datasets may provide potential indications of HD-specific metabolic signatures. In fact, while some alterations can be observed in common between AD and HD, for example global decrease in some neurotransmitter levels, distinct metabolite signatures emerge in HD brains. For instance, whereas polyol pathway-related metabolites, namely glucose, sorbitol and fructose, increase steadily according to the known pathological gradient in AD brain, in HD the accumulation of these metabolites is limited to the putamen and is not heavily influenced by the widespread degeneration occurring in other HD brain regions. The aromatic amino acids tryptophan and tyrosine, which share chorismic acid as their common precursor, seem to be distinctively modulated in HD. In fact, while the tryptophan/tyrosine ratio is approximately in equilibrium in HD brain, whether the region considered undergoes severe degeneration or not, in AD brain this ratio is predominantly weighted towards tryptophan and correlated with disease severity. Finally, scyllo-inositol alterations were solely associated with HD brain in these studies. Taken together, the results of these comparative observations, although purely qualitative at this stage, may indicate variation in metabolite abundances which are perhaps solely associated with HD and which deserves further investigation.

This study has limitations. Suppl. Table 1 provides information including cause of death in controls and cases: this was the primary cause listed on the death certificate. The table includes a column showing the neuropathological grade of each HD case (i.e. Vonsattel Grade), which indicates the degree of caudate-putamen degeneration at the time of death [18]. Six cases whose Vonsattel Grades varied from 1 (mildly affected) to 4 (most severely affected), had bronchopneumonia listed as the cause of death: thus bronchopneumonia was the most frequent cause of death in this group of HD patients and was not related to Vonsattel pathological grade. The age at death varied considerably (between 51 and 83 yrs), as frequently occurs in such patients, although expanded CAG repeat numbers varied between 40 and 47. Due to the insidious nature of the disease, age at onset was not indicated. Vonsattel Grades differed somewhat between brains, which could possibly have weakened correlations for some molecules, so correlations may have been even higher had all brains been at the same stage. The Vonsattel Grades of these HD patients are consistent with varying degrees of degeneration of the caudate-putamen, which displayed early to late pathological grades: however, all of these HD patients demonstrated uniform alterations in different classes of polar metabolites in the striatal portion of the brain (i.e. glucose, sorbitol and fructose). We aimed to identify and map regional alterations in metabolite levels across a large portion of the HD brain, using a strategy based on material with short-*post-mortem* delay. Limitations of such *post-mortem* analyses must therefore be considered. First, we should reflect on the possible effect that PMD could exert on brain metabolites. In fact, although our samples were matched for PMD, and significant associations of PMD with accumulation or reduction of metabolites were not detected by correlational analyses, we cannot completely exclude the possibility that degradation of some metabolites might have occurred in our human-brain samples soon after death: consequently, we cannot establish with certainty how such an artefact might have influenced our analyses. However, the case-control design we employed can be expected to mitigate against this limitation, at least to some extent. Another limitation consists in the relatively small number of cases generally used in *post-mortem* studies. While the number of specimens analysed here (ca. 300) allowed us to establish a robust and reproducible GC–MS workflow for analysis of *post-mortem* brain samples, a follow-up study based on larger cohorts is recommended to validate and extend our initial findings, and eventually to unmask small-to-moderate effect sizes in metabolite abundances. In addition, it is

important to remember that some of the alterations reported in the present study may represent secondary effects caused by an unknown primary mechanism responsible for metabolic alteration in HD. Thus, even if these alterations might be potentially regarded as compensatory or harmful responses potentially linked to the metabolic signature of HD, further studies are necessary to elucidate how the causative HTT mutation is precisely influencing HD metabolism. Finally, it would be of interest to establish at what stage of the disease progression the metabolite alterations described in this study might first occur. Even so, it should be reminded that *post-mortem* human studies have enormously contributed so far to our knowledge about critical aspects of neurodegenerative diseases and drug-design for these disorders [101,102].

5. Conclusion

We have here identified and mapped a widespread pattern of metabolic perturbations in eleven regions of *post-mortem* brain from patients who died with HD. Moreover, several of the metabolite alterations identified here as contributing to the disease signature were found to be correlated with expansion of the causative HD mutation. As the huntingtin protein is ubiquitously expressed in brain but only limited areas are apparently subject to the severe structural consequences of its toxic effects in HD, the region-specific metabolic signatures identified in this study lay the foundations for a better understanding of how the mutant HD protein might cause localised metabolic perturbations in the CNS, and of which molecular mechanisms might be activated in specific regions to counterbalance these perturbations. Ultimately, the need for a better understanding of the mechanisms by which metabolic aberrations exert their influence on HD phenotype is acute. It is hoped that the findings presented here will serve as a useful platform to identify mechanisms suitable for pharmacological targeting to rapidly develop new and effective experimental therapies for HD for translation into the clinic.

Supplementary data to this article can be found online at http://dx.doi.org/10.1016/j.bbadis.2016.06.002.

Author contributions

SP designed and performed research, analysed and interpreted data, and wrote the manuscript; PB designed and performed research, analysed data, and revised the manuscript; JX and SJC performed research and revised the manuscript; SJR and EC revised the manuscript; MC, MD, HJW and RGS performed research and revised the manuscript; RDU designed and interpreted research and wrote the manuscript; RLMF led development of the New Zealand Neurological Foundation Human Brain Bank, supervised brain collection and dissection, and revised the manuscript; GJSC conceived, designed and supervised research, analysed and interpreted data, wrote the manuscript, and bears overall responsibility for the integrity of the study and of the manuscript.

Funding

This work was supported by grants from the Endocore Research Trust [61047]; Cure Huntington's Disease Initiative (CHDI) (A-8247); the Maurice and Phyllis Paykel Trust [3627036; and Travel funding for JX]; Lottery Health New Zealand [3626585; 3702766]; the Maurice Wilkins Centre for Molecular Biodiscovery [through a Tertiary Education Commission grant 9341-3622506; and a Doctoral Scholarship for JX]; the Health Research Council of New Zealand [3338701]; the University of Auckland [Doctoral Student PReSS funding JXU058]; the Oakley Mental Health Research Foundation [3456030; 3627092; 3701339; 3703253; and 3702870]; the Ministry of Business, Innovation & Employment [UOAX0815]; the New Zealand Neurological Foundation; the Medical Research Council [UK; MR/L010445/1 and MR/L011093/1]; Alzheimer's Research UK (ARUK-PPG2014B-7); the University of Manchester, the Central Manchester (NHS) Foundation Trust, and the Northwest Regional Development Agency through a combined programme grant to CADET; and was facilitated by the Manchester Biomedical Research Centre and the Greater Manchester Comprehensive Local Research Network.

Conflict of interest statement

The authors declare that they have no conflict of interest with respect to this work. Sponsors had no role in the study design; the collection, analysis and interpretation of data; the writing of the manuscript; or the decision to submit the article for publication. All data are provided in full in the results section of this paper.

Transparency Document

The Transparency document associated with this article can be found, in online version.

Acknowledgments

We thank all the families of patients with Huntington's disease who so generously supported this research through the donation of brain tissue to the NZ Neurological Foundation Human Brain Bank in the Centre for Brain Research, Faculty of Medical and Health Sciences, University of Auckland, New Zealand. We also thank Marika Eszes, Cynthia Tse and Michael Anderson for their management support.

References

[1] The Huntington's, D., Collaborative, Research, Group, A novel gene containing a trinucleotide repeat that is expanded and unstable on Huntington's disease chromosomes, Cell 72 (6) (1993) 971–983.
[2] F.O. Walker, Huntington's disease, Semin. Neurol. 27 (2) (2007) 143–150.
[3] R.G. Snell, et al., Relationship between trinucleotide repeat expansion and phenotypic variation in Huntington's disease, Nat. Genet. 4 (4) (1993) 393–397.
[4] H.J. Waldvogel, et al., The neuropathology of Huntington's disease, Curr. Top. Behav. Neurosci. 22 (2015) 33–80.
[5] J.B. Martin, J.F. Gusella, Huntington's disease. Pathogenesis and management, N. Engl. J. Med. 315 (20) (1986) 1267–1276.
[6] L. Djousse, et al., Weight loss in early stage of Huntington's disease, Neurology 59 (9) (2002) 1325–1330.
[7] F. Mochel, et al., Abnormal response to cortical activation in early stages of Huntington disease, Mov. Disord. 27 (7) (2012) 907–910.
[8] I.M. Adanyeguh, et al., Triheptanoin improves brain energy metabolism in patients with Huntington disease, Neurology 84 (5) (2015) 490–495.
[9] W. Duan, M. Jiang, J. Jin, Metabolism in HD: still a relevant mechanism? Mov. Disord. 29 (11) (2014) 1366–1374.
[10] L. Yang, et al., Combination therapy with coenzyme Q10 and creatine produces additive neuroprotective effects in models of Parkinson's and Huntington's diseases, J. Neurochem. 109 (5) (2009) 1427–1439.
[11] K.M. Shannon, A. Fraint, Therapeutic advances in Huntington's disease, Mov. Disord. 30 (11) (2015) 1539–1546.
[12] J.B. Carroll, et al., Treating the whole body in Huntington's disease, Lancet Neurol. 14 (11) (2015) 1135–1142.
[13] C.C. Tang, et al., Metabolic network as a progression biomarker of premanifest Huntington's disease, J. Clin. Invest. 123 (9) (2013) 4076–4088.
[14] B.R. Underwood, et al., Huntington disease patients and transgenic mice have similar pro-catabolic serum metabolite profiles, Brain 129 (Pt 4) (2006) 877–886.
[15] R. Nambron, et al., A metabolic study of Huntington's disease, PLoS One 11 (1) (2016), e0146480.
[16] H.J. Waldvogel, et al., The collection and processing of human brain tissue for research, Cell Tissue Bank. 9 (3) (2008) 169–179.
[17] H.J. Waldvogel, et al., Immunohistochemical staining of post-mortem adult human brain sections, Nat. Protoc. 1 (6) (2006) 2719–2732.
[18] J.P. Vonsattel, et al., Neuropathological classification of Huntington's disease, J. Neuropathol. Exp. Neurol. 44 (6) (1985) 559–577.
[19] A. Reiner, I. Dragatsis, P. Dietrich, Genetics and neuropathology of Huntington's disease, Int. Rev. Neurobiol. 98 (2011) 325–372.
[20] P. Begley, et al., Development and performance of a gas chromatography-time-of-flight mass spectrometry analysis for large-scale nontargeted metabolomic studies of human serum, Anal. Chem. 81 (16) (2009) 7038–7046.
[21] W.B. Dunn, et al., Procedures for large-scale metabolic profiling of serum and plasma using gas chromatography and liquid chromatography coupled to mass spectrometry, Nat. Protoc. 6 (7) (2011) 1060–1083.

[22] C.F. Poole, Alkylsilyl derivatives for gas chromatography, J. Chromatogr. A 1296 (2013) 2–14.
[23] Y. Benjamini, Y. Hochberg, Controlling the false discovery rate: a practical and powerful approach to multiple testing, J. R. Stat. Soc. 57 (1) (1995) 289–300.
[24] K. Morgenthal, W. Weckwerth, R. Steuer, Metabolomic networks in plants: transitions from pattern recognition to biological interpretation, Biosystems 83 (2–3) (2006) 108–117.
[25] H.L. Kotze, et al., A novel untargeted metabolomics correlation-based network analysis incorporating human metabolic reconstructions, BMC Syst. Biol. 7 (2013) 107.
[26] E.H. Aylward, et al., Longitudinal change in regional brain volumes in prodromal Huntington disease, J. Neurol. Neurosurg. Psychiatry 82 (4) (2011) 405–410.
[27] H.D. Rosas, et al., Striatal volume loss in HD as measured by MRI and the influence of CAG repeat, Neurology 57 (6) (2001) 1025–1028.
[28] F. Niccolini, M. Politis, Neuroimaging in Huntington's disease, World J. Radiol. 6 (6) (2014) 301–312.
[29] C.A. Ross, et al., Huntington disease: natural history, biomarkers and prospects for therapeutics, Nat. Rev. Neurol. 10 (4) (2014) 204–216.
[30] U. Rub, et al., The neuropathology of Huntington s disease: classical findings, recent developments and correlation to functional neuroanatomy, Adv. Anat. Embryol. Cell Biol. 217 (2015) 1–146.
[31] G. Nicolas, et al., Juvenile Huntington disease in an 18-month-old boy revealed by global developmental delay and reduced cerebellar volume, Am. J. Med. Genet. A 155A (4) (2011) 815–818.
[32] U. Rub, et al., Degeneration of the cerebellum in Huntington's disease (HD): possible relevance for the clinical picture and potential gateway to pathological mechanisms of the disease process, Brain Pathol. 23 (2) (2013) 165–177.
[33] E. Spargo, I.P. Everall, P.L. Lantos, Neuronal loss in the hippocampus in Huntington's disease: a comparison with HIV infection, J. Neurol. Neurosurg. Psychiatry 56 (5) (1993) 487–491.
[34] R.K. Byers, F.H. Gilles, C. Fung, Huntington's disease in children. Neuropathologic study of four cases, Neurology 23 (6) (1973) 561–569.
[35] S.J. Tabrizi, et al., Biochemical abnormalities and excitotoxicity in Huntington's disease brain, Ann. Neurol. 45 (1) (1999) 25–32.
[36] L. Cui, et al., Transcriptional repression of PGC-1alpha by mutant huntingtin leads to mitochondrial dysfunction and neurodegeneration, Cell 127 (1) (2006) 59–69.
[37] T. Milakovic, G.V. Johnson, Mitochondrial respiration and ATP production are significantly impaired in striatal cells expressing mutant huntingtin, J. Biol. Chem. 280 (35) (2005) 30773–30782.
[38] D. Lim, et al., Calcium homeostasis and mitochondrial dysfunction in striatal neurons of Huntington disease, J. Biol. Chem. 283 (9) (2008) 5780–5789.
[39] D.E. Kuhl, et al., Local cerebral glucose utilization in symptomatic and presymptomatic Huntington's disease, Res. Publ. Assoc. Res. Nerv. Ment. Dis. 63 (1985) 199–209.
[40] A. Antonini, et al., Striatal glucose metabolism and dopamine D2 receptor binding in asymptomatic gene carriers and patients with Huntington's disease, Brain 119 (Pt 6) (1996) 2085–2095.
[41] K. Bergbauer, et al., Studies on fructose metabolism in cultured astroglial cells and control hepatocytes: lack of fructokinase activity and immunoreactivity in astrocytes, Dev. Neurosci. 18 (5–6) (1996) 371–379.
[42] J. Xu, et al., Graded perturbations of metabolism in multiple regions of human brain in Alzheimer's disease: snapshot of a pervasive metabolic disorder, Biochim. Biophys. Acta (2016).
[43] S.N. Ho, Intracellular water homeostasis and the mammalian cellular osmotic stress response, J. Cell. Physiol. 206 (1) (2006) 9–15.
[44] D. Voet, J. Voet, in: I. John Wiley & Sons (Ed.), Biochemistry, second ed.Wiley, New York, 1995.
[45] J. Yao, et al., Shift in brain metabolism in late onset Alzheimer's disease: implications for biomarkers and therapeutic interventions, Mol. Asp. Med. 32 (4–6) (2011) 247–257.
[46] L. Dunn, et al., Dysregulation of glucose metabolism is an early event in sporadic Parkinson's disease, Neurobiol. Aging 35 (5) (2014) 1111–1115.
[47] S.H. Stuwe, et al., Hepatic mitochondrial dysfunction in manifest and premanifest Huntington disease, Neurology 80 (8) (2013) 743–746.
[48] R. Hoffmann, et al., Progressive hepatic mitochondrial dysfunction in premanifest Huntington's disease, Mov. Disord. 29 (6) (2014) 831–834.
[49] R.R. Handley, et al., Metabolic disruption identified in the Huntington's disease transgenic sheep model, Sci. Rep. 6 (2016) 20681.
[50] D. Voet, J. Voet, second ed., Biochemistry, vol. II, John Wiley & Sons, New York, 1995.
[51] F. Mochel, et al., Early energy deficit in Huntington disease: identification of a plasma biomarker traceable during disease progression, PLoS One 2 (7) (2007), e647.
[52] D. Ebert, R.G. Haller, M.E. Walton, Energy contribution of octanoate to intact rat brain metabolism measured by ^{13}C nuclear magnetic resonance spectroscopy, J. Neurosci. 23 (13) (2003) 5928–5935.
[53] M. He, et al., Identification and characterization of new long chain acyl-CoA dehydrogenases, Mol. Genet. Metab. 102 (4) (2011) 418–429.
[54] A. Panov, et al., Fatty acids in energy metabolism of the central nervous system, Biomed. Res. Int. 2014 (2014) 472459.
[55] N.N. Naseri, et al., Abnormalities in the tricarboxylic acid cycle in Huntington disease and in a Huntington disease mouse model, J. Neuropathol. Exp. Neurol. 74 (6) (2015) 527–537.
[56] S. Patassini, et al., Identification of elevated urea as a severe, ubiquitous metabolic defect in the brain of patients with Huntington's disease, Biochem. Biophys. Res. Commun. 468 (1–2) (2015) 161–166.
[57] A. Hodges, et al., Regional and cellular gene expression changes in human Huntington's disease brain, Hum. Mol. Genet. 15 (6) (2006) 965–977.
[58] C.A. Colton, et al., Disrupted spermine homeostasis: a novel mechanism in polyglutamine-mediated aggregation and cell death, J. Neurosci. 24 (32) (2004) 7118–7127.
[59] A.T. van der Goot, E.A. Nollen, Tryptophan metabolism: entering the field of aging and age-related pathologies, Trends Mol. Med. 19 (6) (2013) 336–344.
[60] J.R. Moffett, M.A. Namboodiri, Tryptophan and the immune response, Immunol. Cell Biol. 81 (4) (2003) 247–265.
[61] G.F. Oxenkrug, Metabolic syndrome, age-associated neuroendocrine disorders, and dysregulation of tryptophan-kynurenine metabolism, Ann. N. Y. Acad. Sci. 1199 (2010) 1–14.
[62] E.M. Gal, A.D. Sherman, Synthesis and metabolism of L-kynurenine in rat brain, J. Neurochem. 30 (3) (1978) 607–613.
[63] C.M. Forrest, et al., Blood levels of kynurenines, interleukin-23 and soluble human leucocyte antigen-G at different stages of Huntington's disease, J. Neurochem. 112 (1) (2010) 112–122.
[64] N. Stoy, et al., Tryptophan metabolism and oxidative stress in patients with Huntington's disease, J. Neurochem. 93 (3) (2005) 611–623.
[65] O.T. Phillipson, E.D. Bird, Plasma glucose, non-esterified fatty acids and amino acids in Huntington's chorea, Clin. Sci. Mol. Med. 52 (3) (1977) 311–318.
[66] M.F. Beal, et al., Kynurenine pathway measurements in Huntington's disease striatum: evidence for reduced formation of kynurenic acid, J. Neurochem. 55 (4) (1990) 1327–1339.
[67] J.O. Ottosson, W. Rapp, Serum levels of phenylalanine and tyrosine in Huntington's chorea, Acta Psychiatr. Scand. Suppl. 221 (1971) 89-1.
[68] R.A. Williams, C.D. Mamotte, J.R. Burnett, Phenylketonuria: an inborn error of phenylalanine metabolism, Clin. Biochem. Rev. 29 (1) (2008) 31–41.
[69] L. Adler-Abramovich, et al., Phenylalanine assembly into toxic fibrils suggests amyloid etiology in phenylketonuria, Nat. Chem. Biol. 8 (8) (2012) 701–706.
[70] E.L. Macleod, D.M. Ney, Nutritional management of phenylketonuria, Ann. Nestle Eng. 68 (2) (2010) 58–69.
[71] H.D. Rosas, et al., A systems-level "misunderstanding": the plasma metabolome in Huntington's disease, Ann. Clin. Transl. Neurol. 2 (7) (2015) 756–768.
[72] P.S. Sastry, Lipids of nervous tissue: composition and metabolism, Prog. Lipid Res. 24 (2) (1985) 69–176.
[73] F. Gibellini, T.K. Smith, The Kennedy pathway–de novo synthesis of phosphatidylethanolamine and phosphatidylcholine, IUBMB Life 62 (6) (2010) 414–428.
[74] D.W. Ellison, M.F. Beal, J.B. Martin, Phosphoethanolamine and ethanolamine are decreased in Alzheimer's disease and Huntington's disease, Brain Res. 417 (2) (1987) 389–392.
[75] R. Smith, P. Brundin, J.Y. Li, Synaptic dysfunction in Huntington's disease: a new perspective, Cell. Mol. Life Sci. 62 (17) (2005) 1901–1912.
[76] M. Katsuno, H. Adachi, G. Sobue, Getting a handle on Huntington's disease: the case for cholesterol, Nat. Med. 15 (3) (2009) 253–254.
[77] R. Truant, R. Atwal, A. Burtnik, Hypothesis: huntingtin may function in membrane association and vesicular trafficking, Biochem. Cell Biol. 84 (6) (2006) 912–917.
[78] L. Yang, M.F. Beal, Determination of neurotransmitter levels in models of Parkinson's disease by HPLC-ECD, Methods Mol. Biol. 793 (2011) 401–415.
[79] D.W. Ellison, et al., Amino acid neurotransmitter abnormalities in Huntington's disease and the quinolinic acid animal model of Huntington's disease, Brain 110 (Pt 6) (1987) 1657–1673.
[80] T.L. Perry, S. Hansen, M. Kloster, Huntington's chorea. Deficiency of gamma-aminobutyric acid in brain, N. Engl. J. Med. 288 (7) (1973) 337–342.
[81] N. Ando, et al., Regional brain levels of gamma-hydroxybutyrate in Huntington's disease, J. Neurochem. 32 (2) (1979) 617–622.
[82] A.Y. Lai, J. McLaurin, Inhibition of amyloid-beta peptide aggregation rescues the autophagic deficits in the TgCRND8 mouse model of Alzheimer disease, Biochim. Biophys. Acta 1822 (10) (2012) 1629–1637.
[83] K. Vekrellis, et al., Inducible over-expression of wild type alpha-synuclein in human neuronal cells leads to caspase-dependent non-apoptotic death, J. Neurochem. 109 (5) (2009) 1348–1362.
[84] A.Y. Lai, et al., Scyllo-Inositol promotes robust mutant Huntingtin protein degradation, J. Biol. Chem. 289 (6) (2014) 3666–3676.
[85] S.K. Fisher, J.E. Novak, B.W. Agranoff, Inositol and higher inositol phosphates in neural tissues: homeostasis, metabolism and functional significance, J. Neurochem. 82 (4) (2002) 736–754.
[86] A. Bitsch, et al., Inflammatory CNS demyelination: histopathologic correlation with in vivo quantitative proton MR spectroscopy, AJNR Am. J. Neuroradiol. 20 (9) (1999) 1619–1627.
[87] D. Yang, et al., Volumetric MRI and MRS provide sensitive measures of Alzheimer's disease neuropathology in inducible Tau transgenic mice (rTg4510), NeuroImage 54 (4) (2011) 2652–2658.
[88] R.J. Maddock, M.H. Buonocore, MR spectroscopic studies of the brain in psychiatric disorders, Curr. Top. Behav. Neurosci. 11 (2012) 199–251.
[89] A. Sturrock, et al., A longitudinal study of magnetic resonance spectroscopy Huntington's disease biomarkers, Mov. Disord. 30 (3) (2015) 393–401.
[90] S.J. van den Bogaard, et al., Exploratory 7-Tesla magnetic resonance spectroscopy in Huntington's disease provides in vivo evidence for impaired energy metabolism, J. Neurol. 258 (12) (2011) 2230–2239.
[91] K. Strange, et al., Osmoregulatory changes in myo-inositol content and Na+/myo-inositol cotransport in rat cortical astrocytes, Glia 12 (1) (1994) 35–43.
[92] T.M. Tsang, et al., Metabolic characterization of the R6/2 transgenic mouse model of Huntington's disease by high-resolution MAS ^{1}H NMR spectroscopy, J. Proteome Res. 5 (3) (2006) 483–492.

[93] K. Strange, et al., Upregulation of inositol transport mediates inositol accumulation in hyperosmolar brain cells, Am. J. Phys. 260 (4 Pt 1) (1991) C784–C790.
[94] K. Strange, R. Morrison, Volume regulation during recovery from chronic hypertonicity in brain glial cells, Am. J. Phys. 263 (2 Pt 1) (1992) C412–C419.
[95] M.D. Norenberg, et al., Ammonia-induced astrocyte swelling in primary culture, Neurochem. Res. 16 (7) (1991) 833–836.
[96] D. Haussinger, et al., Proton magnetic resonance spectroscopy studies on human brain myo-inositol in hypo-osmolarity and hepatic encephalopathy, Gastroenterology 107 (5) (1994) 1475–1480.
[97] J. Laubenberger, et al., Proton magnetic resonance spectroscopy of the brain in symptomatic and asymptomatic patients with liver cirrhosis, Gastroenterology 112 (5) (1997) 1610–1616.
[98] R.A. Moats, et al., Decrease in cerebral inositols in rats and humans, Biochem. J. 295 (Pt 1) (1993) 15–18.
[99] R.A. Moats, et al., Abnormal cerebral metabolite concentrations in patients with probable Alzheimer disease, Magn. Reson. Med. 32 (1) (1994) 110–115.
[100] M.C. Chiang, et al., Dysregulation of C/EBPalpha by mutant Huntingtin causes the urea cycle deficiency in Huntington's disease, Hum. Mol. Genet. 16 (5) (2007) 483–498.
[101] H. Kretzschmar, Brain banking: opportunities, challenges and meaning for the future, Nat. Rev. Neurosci. 10 (1) (2009) 70–78.
[102] T.G. Beach, Alzheimer's disease and the “Valley Of Death”: not enough guidance from human brain tissue? J. Alzheimers Dis. 33 (Suppl. 1) (2013) S219–S233.